A Fifth-Order-Accurate Finite Difference Scheme for a Natural Coordinate System with Non-Uniform Grid

IDRIS GADOURA
Department of Engineering
University of New Brunswick
100 Tucker Park Road, Saint John, New Brunswick, E2L 4L5
CANADA

M.H. HAMDAN
Department of Mathematics and Statistics
University of New Brunswick
100 Tucker Park Road, Saint John, New Brunswick, E2L 4L5
CANADA

Abstract: - A fifth-order accurate finite difference scheme for the first derivative in von Mises coordinates is developed in this work. The scheme is tested in the computation of boundary vorticity in the study of two-dimensional flow of a viscous fluid in a curvilinear channel. Results obtained show an improvement in the computed solution over fourth-order accurate scheme.

Key-Words: - von Mises natural coordinates, Non-uniform grid, Fifth-order scheme.

Received: July 15, 2021. Revised: February 18, 2022. Accepted: March 12, 2022. Published: April 19, 2022.

1 Introduction

A large amount of research has been devoted to the development and testing of higher order finite difference schemes when a non-uniform grid is employed (*c.f.* [1,2,3,4] and the references therein). In two-dimensional viscous fluid flow, the Navier-Stokes equations in vorticity-streamfunction form are approximated using second-order central differencing schemes. On a solid boundary, the streamfunction equation possesses Dirichlet conditions while the vorticity equation possesses Neumann conditions, hence vorticity must be computed on the boundary. A further aspect to handle is when the flow is through a curvilinear domain and the numerical procedure of choice is the finite difference approach. In this case it becomes necessary to transform the physical domain onto a computational domain prior to applying finite differences. While there are many methods of transforming a curvilinear domain onto a rectangular one, a transformation of interest to the current work is the von Mises transformation, as it presents itself as a natural coordinate transformation with physical significance and connection to the streamlines of the flow, [5-6].

In using the von Mises transformation, the curvilinear physical domain in the XY-plane is transformed onto a rectangular computational domain in the $X\psi$-plane, where ψ is the streamfunction and $\psi = constant$ represent the streamlines of the flow, provided that the boundary is a streamline or part of a streamline of the flow. The governing equations in vorticity-streamfunction form in the physical domain are transformed into a vorticity equation and an equation for $y(x, \psi)$ in the computational domain. Similarly, all physical boundary conditions are transformed into computational boundary conditions, and the vorticity derivative boundary conditions in the physical domain are transformed into vorticity derivative boundary conditions in von Mises coordinates. Vorticity at the computational domain boundaries remains a quantity to be determined (approximated) using finite differences.

It has been argued that a higher-order scheme for the vorticity on a solid wall may better approximate the vorticity there. Some authors, [7-9], suggested that the accuracy of the solution to the governing equations depends not only on the order of the scheme; rather, other factors such as the stretching parameters, the tolerance used in the solution procedure, and the actual iterative procedure should be taken into consideration. Higher-order schemes have been shown to produce better approximations to boundary vorticity. In fact, in the work of Alharbi and Hamdan, [10], a fourth-order accurate scheme for non-uniform grid was developed for the problem considered in this work and produced better boundary vorticity approximations than lower-order schemes.

This motivates the current work in which we develop a standard, six-point, fifth-order-accurate forward finite difference scheme for the boundary vorticity using non-uniform grids. The scheme is suitable for use when coordinate transformation is employed, and is tested in the computation of corner vorticity in the case of viscous fluid flow through a two-dimensional curvilinear channel that has been mapped onto a rectangular computational domain using von Mises coordinates. Results show the improvement in boundary vorticity approximation.

2 Problem Formulation

Consider the viscous fluid flow in the curvilinear (long) channel depicted in **Fig.** 1, below, described by $\{(x,y)|a \le x \le b;\ g_1(x) \le y \le g_2(x)\}$, where $g_1(x)$and $g_2(x)$ are known smooth functions. The inlet to the channel is $-1 \le y \le 1$. Flow through the channel is governed by the Navier-Stokes equations, in vorticity-streamfunction form, with boundary conditions on vorticity ω and streamfunction ψ as shown in **Fig.** 1, (*cf.* [1] for more details).

At the inlet, the tangential velocity profile is parabolic, $u = 1 - y^2$, and the normal velocity $v = 0$. The square of the speed of the flow is $q^2 = u^2 + v^2 = [1 - y^2]^2$. Vorticity at the inlet to the channel is given by $\omega = 2y$. At the point $(x,y) = (a,-1)$, vorticity takes the value $\omega = -2$. The streamfunction at the inlet to the channel is given by $\psi = y - \frac{y^3}{3}$ for $y_{min} = -1 \le y \le 1 = y_{max}$.The streamlines thus range between the minimum and maximum values $\psi = \psi_{min} = -\frac{2}{3}$ and $\psi = \psi_{max} = \frac{2}{3}$.

In the absence of an exact solution to the given problem, it is typical to use a numerical technique, such as finite differences. The presence of curvilinear boundaries, however, necessitates mapping the flow domain onto a rectangular computational domain. To accomplish this, we rely on the well-known von Mises transformation, $(x,y) \to (x,\psi)$, defined by $y = y(x,\psi)$. In the curvilinear net (x,ψ), the curves $\psi = constant$ represent the streamlines of the flow. Jacobian of the von Mises transformation is given by $J = \left|\frac{\partial(x,y)}{\partial(x,\psi)}\right| = y_\psi$. If $0 < J < \infty$, then the inverse transformation exists and we can relate first partial derivative operators in the two coordinate systems as follows, wherein subscript notation denotes partial differentiation, [6]:

$$\partial_x = \partial_x - \frac{y_x}{y_\psi}\partial_\psi \tag{1}$$

$$\partial_y = \frac{1}{y_\psi}\partial_\psi \tag{2}$$

Velocity components and vorticity take the following forms, respectively, in von Mises coordinates:

$$u = \frac{1}{y_\psi} \tag{3}$$

$$v = \frac{y_x}{y_\psi} = u y_x \tag{4}$$

$$\omega = v_x + \left(\frac{v^2}{u} - u\right)u_\psi - \frac{v}{u}u_x - 2vv_\psi \tag{5}$$

The square of the speed of the flow is given by

$$q^2 = u^2 + v^2 = \frac{1+(y_x)^2}{(y_\psi)^2} \tag{6}$$

Vorticity, (6), can thus be written in terms of the square of the speed, $q^2 = u^2 + v^2$, as

$$\omega = v_x - \frac{1}{2}(q^2)_\psi \tag{7}$$

In the problem at hand, $v_x = 0$ on all boundaries, and equation (7) reduces to:

$$\omega = -\frac{1}{2}(q^2)_\psi \tag{8}$$

DOI: 10.37394/232021.2022.2.5

The physical domain, **Fig. 1**, is this transformed onto the computational domain shown in **Fig. 2**.

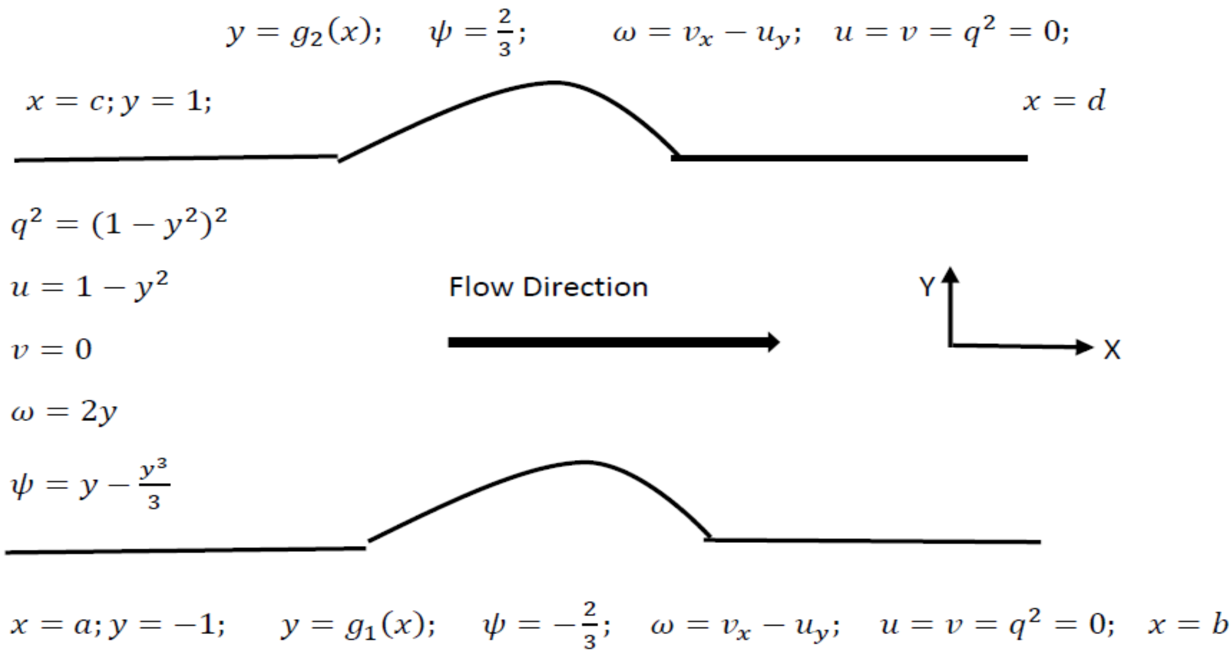

Fig. 1 Physical Flow Configuration

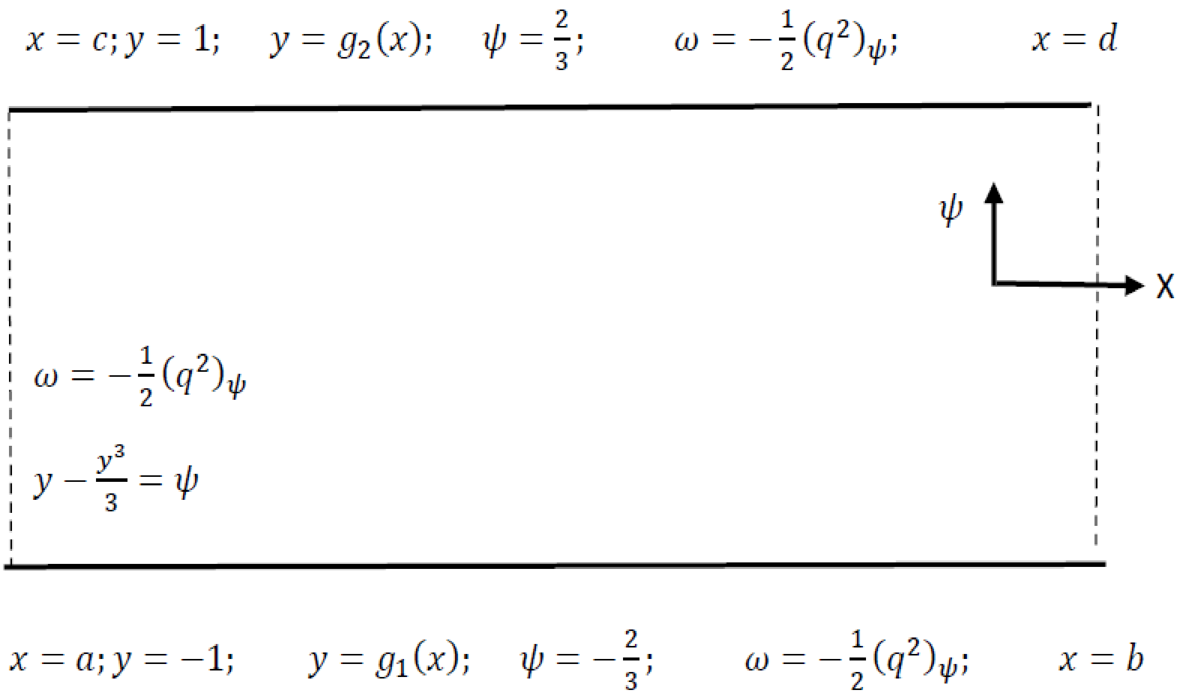

Fig. 2 Computational Domain

3 Current Objectives

The objective of the current work is to derive a fifth-order-accurate forward difference scheme for $(q^2)_\psi$ of equation (8) that uses six grid points, one boundary point and five internal infield points, using Taylor series expansion. The scheme will be used to compute the vorticity at a boundary point where the exact solution is known, namely $\omega(x,\psi) = -2$ at $x = 0$ and $\psi = -\frac{2}{3}$. The developed scheme is an upwind, forward differencing scheme that can be used to approximate lower boundary vorticity. A backward differencing scheme can be then deduced and used in approximating vorticity on the upper boundary.

Fitth-order scheme is derived below for non-uniform grid in the computational domain. However, we point out the following caveat. If a uniform grid is used in the physical domain, then the von Mises coordinate system naturally produces a grid that is clustered near the boundary. This effect is desired for more accurate results. However, if a uniform grid is chosen in the computational domain, then the physical domain grid is clustered near the centre of the channel and far away from the boundary. This effects is not desired as it produces less accurate results by not capturing the effects of boundary vorticity on the flow, as would a clustered grid.

4 Domain Discretization

In order to accomplish the above objective, the rectangular computational domain of **Fig. 2** is discretized using a non-uniform, clustered grid by taking vertical grid lines to range from *i=1* at channel inlet to *i=Imax* at channel exit. Horizontal grid lines are taken to range from *j=1* at the lower computational boundary, ($\psi = -\frac{2}{3}$), to *j=Jmax* at the upper computational boundary, ($\psi = \frac{2}{3}$), as shown in **Fig. 3**.

For non-uniform grid, we select a uniform grid in the physical domain with 200 points in the y-direction, resulting in step size $\Delta y = \frac{y_{max}-y_{min}}{200} = \frac{[1-(-1)]}{200} = 0.01$. Grid spacings $\Delta\psi_j$ are then calculated in the computational domain using $y - \frac{y^3}{3} = \psi$ for $-\frac{2}{3} \le \psi \le \frac{2}{3}$. These are shown in **Table 1**.

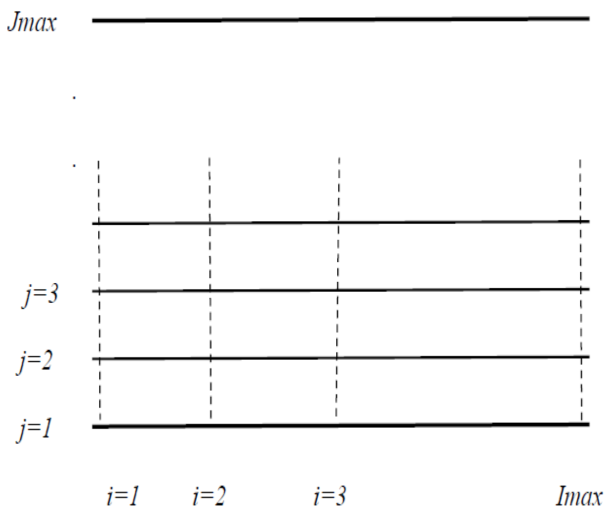

Fig. 3. Grid Lines. *(i,j)=(1,1)* Corresponds to *(x,y)=(a,-1)*

5 Derivation of the Scheme

In order to derive forward differencing schemes of local accuracy *n* for the first derivative along the grid line $(i,1)$using $k_{max} = 6$ grid points, where the scheme will employ one boundary point and five internal grid points, namely grid points *j=1, 2, 3, 4, 5* and *6*, we assume the schemes to be of the form, [8]:

$$\left(q_\psi^2\right)_{i,1} + \sum_{j=1}^{6} A_j (q^2)_{i,j} = E \tag{9}$$

where *E* is the local truncation error.

The weights, A_j, are calculated using Taylor's series expansion of $(q^2)_{i,m}$ about point $(i,1)$ for $m = 2,3,\ldots k_{max} = 6$, namely

$$(q^2)_{i,m} = \sum_{j=1}^{5} \frac{(a_m)^{j-1}}{(j-1)!} \frac{\partial^{j-1} q^2}{\partial\psi^{j-1}}\Big|_{(i,1)} + E_6 \tag{10}$$

$$E_6 = \sum_{j=6}^{\infty} \frac{(a_m)^{j-1}}{(j-1)!} \frac{\partial^{j-1} q^2}{\partial\psi^{j-1}}\Big|_{(i,1)} \tag{11}$$

The coefficients a_m, $m = 2,3,\ldots,k_{max} = 6$ are defined by

$$a_m = \sum_{j=1}^{m-1} \Delta\psi_j \tag{12}$$

$$\Delta\psi_j = \psi_{j+1} - \psi_j \tag{13}$$

j	y_j^*	$y_j = -y_j^*$	$\Delta y_j = y_{j+1} - y_j$	ψ_j	$\Delta\psi_j = \psi_{j+1} - \psi_j$
1	1	$y_1 = -1$	0.01	$\psi_1 = -0.666666666$	$\Delta\psi_1 = 0.000099666$
2	0.99	$y_2 = -0.99$	0.01	$\psi_2 = -0.666567000$	$\Delta\psi_2 = 0.000297667$
3	0.98	$y_3 = -0.98$	0.01	$\psi_3 = -0.666269333$	$\Delta\psi_3 = 0.000493667$
4	0.97	$y_4 = -0.97$	0.01	$\psi_4 = -0.665775666$	$\Delta\psi_4 = 0.000687666$
5	0.96	$y_5 = -0.96$	0.01	$\psi_5 = -0.665088000$	$\Delta\psi_5 = 0.000879667$
6	0.95	$y_6 = -0.95$		$\psi_6 = -0.664208333$	

Table 1: Grid in the Physical Domain
$y_j = -y_j^*$ for y_j^* =1,0.99,0.98,0.97,0.96,0.95

Values of $\Delta\psi_j$ were provided in **Table 1**, and the square of the speed at channel inlet is tabulated in **Table 2.** The corresponding values of a_m are calculated using (12) and (13), and are given in **Table 3**.

j	y_j	$q_j^2 = (1 - y_j^2)^2$
1	$y_1 = -1$	0
2	$y_2 = -0.99$	0.00039601
3	$y_3 = -0.98$	0.00156816
4	$y_4 = -0.97$	0.00349281
5	$y_5 = -0.96$	0.00614656
6	$y_6 = -0.95$	0.00950625

Table 2: Square of the Speed at Inlet

a_m	**Value**
$a_2 = \Delta\psi_1$	0.000099666
$a_3 = \Delta\psi_1 + \Delta\psi_2$	0.000397333
$a_4 = \Delta\psi_1 + \Delta\psi_2 + \Delta\psi_3$	0.000891
$a_5 = \Delta\psi_1 + \Delta\psi_2 + \Delta\psi_3 + \Delta\psi_4$	0.001578666
$a_6 = \Delta\psi_1 + \Delta\psi_2 + \Delta\psi_3 + \Delta\psi_4 + \Delta\psi_5$	0.002458333

Table 3. Values of a_m for Non-Uniform Grid

Using (10) in (9) and equating to zero the coefficients of the first *n* partial derivatives (including the zero'th derivative) of q^2 with respect to ψ leads to the following six conditions on A_j, $j = 1,2,\dots,k_{max} = 6$:

$$\sum_{j=1}^{k_{max}=6} A_j = 0 \quad (14)$$

$$\sum_{j=2}^{k_{max}=6} a_j A_j = -1 \quad (15)$$

$$\sum_{j=2}^{k_{max}=6} \frac{(a_j)^m}{m!} A_j = 0; \;\; m = 2,3,4,\ldots \quad (16)$$

Equations (14)-(16) translate into the following six equations in the six coefficients $A_1, A_2, A_3, A_4, A_5, A_6$:

$$A_1 + A_2 + A_3 + A_4 + A_5 + A_6 = 0 \quad (17)$$

$$a_2 A_2 + a_3 A_3 + a_4 A_4 + a_5 A_5 + a_6 A_6 = -1 \quad (18)$$

$$\frac{a_2^2}{2} A_2 + \frac{a_3^2}{2} A_3 + \frac{a_4^2}{2} A_4 + \frac{a_5^2}{2} A_5 + \frac{a_6^2}{2} A_6 = 0 \quad (19)$$

$$\frac{a_2^3}{6} A_2 + \frac{a_3^3}{6} A_3 + \frac{a_4^3}{6} A_4 + \frac{a_5^3}{6} A_5 + \frac{a_6^3}{6} A_6 = 0 \quad (20)$$

$$\frac{a_2^4}{24} A_2 + \frac{a_3^4}{24} A_3 + \frac{a_4^4}{24} A_4 + \frac{a_5^4}{24} A_5 + \frac{a_6^4}{24} A_6 = 0 \quad (21)$$

$$\frac{a_2^5}{120} A_2 + \frac{a_3^5}{120} A_3 + \frac{a_4^5}{120} A_4 + \frac{a_5^5}{120} A_5 + \frac{a_6^5}{120} A_6 = 0 \quad (22)$$

Solution to (17)-(22) takes the following forms in terms of a_m, obtained using **MATLAB** *Symbolic Software:*

$$A_1 = \frac{1}{a_6} + \frac{1}{a_5} + \frac{1}{a_4} + \frac{1}{a_3} + \frac{1}{a_2} \quad (23)$$

$$A_2 = -\frac{a_3 a_4 a_5 a_6}{a_2(a_2-a_3)(a_2-a_4)(a_2-a_5)(a_2-a_6)} \quad (24)$$

$$A_3 = \frac{a_2 a_4 a_5 a_6}{a_3(a_2-a_3)(a_3-a_4)(a_3-a_5)(a_3-a_6)} \quad (25)$$

$$A_4 = -\frac{a_2 a_3 a_5 a_6}{a_4(a_2-a_4)(a_3-a_4)(a_4-a_5)(a_4-a_6)} \quad (26)$$

$$A_5 = \frac{a_2 a_3 a_4 a_6}{a_5(a_2-a_5)(a_3-a_5)(a_4-a_5)(a_5-a_6)} \quad (27)$$

$$A_6 = -\frac{a_2 a_3 a_4 a_5}{a_6(a_2-a_6)(a_3-a_6)(a_4-a_6)(a_5-a_6)} \quad (28)$$

Using (12), we can write (23)-(28) in terms of $\Delta\psi_j$ as:

$$A_1 = \sum_{i=1}^{5} \frac{1}{\sum_{j=1}^{i} \Delta\psi_j} \quad (29)$$

$$A_2 = -\frac{1}{\Delta\psi_1} \frac{\prod_{i=1}^{4} \sum_{j=1}^{i+1} \Delta\psi_j}{\prod_{i=1}^{4} \sum_{j=2}^{i+1} \Delta\psi_j} \quad (30)$$

$$A_3 = \frac{\Delta\psi_1 \prod_{i=3}^{5} \sum_{j=1}^{i} \Delta\psi_j}{(\Delta\psi_1 + \Delta\psi_2)(\Delta\psi_2) \prod_{i=3}^{5} \sum_{j=3}^{i} \Delta\psi_j} \quad (31)$$

$$A_4 = -\frac{\prod_{i=0}^{4} \sum_{j=1}^{i+1} \Delta\psi_j}{\left(\sum_{j=1}^{3} \Delta\psi_j\right)\left(\prod_{i=1}^{3} \sum_{j=i}^{3} \Delta\psi_j\right)\left(\prod_{i=4}^{5} \sum_{j=4}^{i} \Delta\psi_j\right)} \quad (32)$$

$$A_5 = \frac{\Delta\psi_5 \prod_{i=0}^{2} \sum_{j=1}^{i+1} \Delta\psi_j + \prod_{i=0}^{3} \sum_{j=1}^{i+1} \Delta\psi_j}{\Delta\psi_5 \prod_{i=1}^{4} \sum_{j=i}^{4} \Delta\psi_j} \quad (33)$$

$$A_6 = -\frac{\prod_{i=0}^{3} \sum_{j=1}^{i+1} \Delta\psi_j}{\prod_{i=1}^{5} \sum_{j=i}^{5} \Delta\psi_j} \quad (34)$$

6 Results and Discussion

Values of the six coefficients $A_1, A_2, A_3, A_4, A_5, A_6$ are listed in **Table 4**, below. They correspond to non-uniform grid data of **Tables 1** and **3**.

A_j	**Value**
A_1	14,712.853
A_2	−16,776.0981
A_3	2,424.29769
A_4	−409.658693
A_5	51.986845
A_6	−3.380685

Table 4. Values of Coefficients $A_1, A_2, A_3, A_4, A_5, A_6$.

The fifth order accurate finite differences scheme for the first derivative $\left(q_\psi^2\right)_{i,1}$ is provided by equation (9), written as:

$$\left(q_\psi^2\right)_{i,1} \approx -\{A_1(q^2)_{i,1} + A_2(q^2)_{i,2} + A_3(q^2)_{i,3} + A_4(q^2)_{i,4} + A_5(q^2)_{i,5} + A_6(q^2)_{i,6}\} \quad (35)$$

where the coefficients $A_1, A_2, A_3, A_4, A_5, A_6$ are given by (29)-(34) for non-uniform grid.

Using the data of **Tables 2** and **4**, expression (36) renders the following value for $\left(q_\psi^2\right)_{1,1}$:

$$\left(q_\psi^2\right)_{1,1} \approx 3.98527329923628279.$$

Vorticity at the point $(x, y) = (a, -1)$ is obtained by substituting $\left(q_{\psi}^{2}\right)_{1,1}$ in equation (8), as:

$$\omega_{1,1} = -1.992636649618141395.$$

Since the true value is $\omega_{1,1} = -2$, the percentage relative error $(P.R.E.)$, defined as

$$P.R.E. = \left|\frac{True\ quantity - Computed\ quantity}{True\ quantity}\right| \% \quad (36)$$

yields $P.R.E. \approx 0.368\%$.

By comparison with results obtained from first-order accurate to fourth-order accurate schemes, [7], [8], [10], **Table 5** shows that the fifth-order scheme renders the lowest *P.R.E.*

	$\omega_{1,1}$	*P.R.E.*
1st order scheme	−1.9867357	0.666%
2nd order scheme	−1.9911322	0.443%
3rd order scheme	−1.9920387	0.398%
4th order scheme	−1.9924314	0.378%
5th order scheme	−1.9926366	0.368%

Table 5. Comparison of Computed Corner Vorticity

The fifth-order scheme developed in this work is expected to work well with both uniform and clustered grids. Typically, uniform grid in the physical domain is chosen such that $y_j = -y_j^*$ for uniformly varying values of y_j^*. Non-uniform grid in the physical domain can be accomplished in various ways, including the use of elementary functions such as $y_j = -\sqrt{y_j^*}$, $y_j = -\sqrt[3]{y_j^*}$, and $y_j = -(y_j^*)^2$, for uniformly varying values of y_j^*. These functions produce different clustering near the flow domain boundaries, as discussed in [1]. In using these functions, Hamdan, [1], showed that in a fourth-order accurate scheme, they produce results closer to the actual solutions. Similar conclusions are expected in using the current fifth order scheme.

7 Conclusion

A fifth-order accurate finite difference scheme was developed in this work for use with transformed curvilinear coordinates. Non-uniform grid was used as it produced clustering near the boundaries in order to capture effects of the boundary. Scheme was used in computing corner vorticity. The fifth order accurate scheme developed I this work produced the most accurate results so far. In future work, focus will be on developing arbitrary order schemes for non-uniform grid.

References:

[1] Hamdan, M.H., Effects of Physical Coordinate Clustering on Boundary Vorticity Approximations in von Mises Coordinates, *WSEAS Transactions on Fluid Mechanics,* Vol. 16, 2021, pp. 201-213.

[2] Pandit, S.K., Kalita, J.C. and Dalal, D.C., A Fourth Order Accurate Compact Scheme for the Solution of Steady Navier-Stokes Equations on Nonuniform grids, *Computers and Fluids,* Vol. 37(2), 2008, pp. 121-134.

[3] Castillo, J.E., Hyman, J.M., Shashkov, J.M. and Steinberg, S., The Sensitivity and Accuracy of Fourth Order Finite-Difference Schemes on Non-uniform Grids in One Dimension, *Computers and Mathematics with Applications*, Vol. 30(8), 1995, pp. 41-55.

[4] de Rivas, E.K., On the Use of Non-uniform Grids in Finite-Difference Equations, *J. Computational Physics,* Vol. 10(2), 1972, pp. 202-210.

[5] Hamdan, M.H., Natural Coordinate System Approach to Coupled n-phase Fluid Flow in Curved Domains, *Applied Math.and Computation*, Vol. 85(2-3), 1997, 297-304.

[6] Hamdan, M.H., Recent Developments in the von Mises Transformation and its Applications in the Computational Sciences: Plenary Lecture. *In*: *Mathematical Methods, System Theory and Control*, Eds. L. Perlovsky *et.al.*, *MAMECTIS 09*, 2009, pp. 180-189.

[7] Siyyam, H.I., Ford, R.A. and Hamdan, M.H., First-order Accurate Finite Difference Schemes for Boundary Vorticity Approximations in Curvilinear Geometries, *Applied Math. and Computation,* Vol. 215, 2009, pp. 2378-2387.

[8] Awartani, M.M., Ford, R.A. and Hamdan, M.H., Computational Complexities and Streamfunction Coordinates, *Applied Math. and Computation*, Vol. 169(2), 2005, pp. 758-777.

[9] Agarwal, R.K., A Third-order-accurate Upwind Scheme for Navier-Stokes Solutions in Three Dimensions, In: *Computers in flow predictions and fluid dynamics experiments; Proceedings of the Winter Annual Meeting, Washington, DC, American Society of Mechanical Engineers,* (A82-29001 13-02), 1981), pp. 73-82.

[10] Alharbi, S.O. and Hamdan, M.H., High-order Finite Difference Schemes for the First Derivative in von Mises Coordinates, *Journal of Applied Mathematics and Physics*, Vol. 4, 2017, pp. 524-545.

Contribution of individual authors

Both authors conducted literature survey.
M.H. formulated the problem and provided analysis.
Simulation and MATLAB work was conducted by I.G.

Sources of funding
This work has not received any funding from any source.